Optical Materials 34 (2012) 845–849

Contents lists available at SciVerse ScienceDirect

Optical Materials

journal homepage: www.elsevier.com/locate/optmat

Optical properties of Sm^{3+} doped Mg:$LiNbO_3$ and Zn:$LiNbO_3$ single crystals

Yunhua Wang, Biao Wang *, Dong Wu, Shaopeng Lin, Zifan Zhou, Yonzhong Zhu

School of Physics and Engineering, Sun Yat-sen University, Guangzhou 510275, China

ARTICLE INFO

Article history:
Received 7 March 2011
Received in revised form 9 November 2011
Accepted 23 November 2011
Available online 24 December 2011

Keywords:
Sm:Mg:$LiNbO_3$ crystal
Sm:Zn:$LiNbO_3$ crystal
Optical properties
J–O theory
Lifetimes
Emission

ABSTRACT

Sm^{3+} doped Mg:$LiNbO_3$ and Zn:$LiNbO_3$ are grown by Czochralski method. Optical transmittance and emission spectra are measured and Judd–Ofelt theory is applied to determine phenomenological intensity parameters, oscillator strengths, radiant transition rates, total radiant lifetimes, and branching ratios. The calculations show that Judd–Ofelt parameters with the relation of $\Omega_4 > \Omega_2 > \Omega_6$ exist, and $\Sigma\Omega_\xi$ ($\xi = 2$, 4 and 6) in Sm:Zn:$LiNbO_3$ decreases. Fluorescence spectra indicate that visible fluorescence of Sm^{3+} is made up of 570, 606, 613 and 654 nm emission bands in these crystals under 409 nm excitation.

1. Introduction

With electro-optic and nonlinear optical characterization, $LiNbO_3$ (LN) single crystal has been investigated and applied as optoelectronic devices such as optical parametric oscillators, optical switches, optical waveguides and frequency doubling [1–3]. Rear earth ions are served as active ions for laser materials because of their good luminescent properties. Lanthanide trivalent rare earth ions in the host of $LiNbO_3$ are investigated including Pr^{3+}, Dy^{3+}, Ho^{3+}, Er^{3+}, Tb^{3+}, Yb^{3+}, Nd^{3+} and Tm^{3+} [4–15], wide host transparency and non-linear properties present that $LiNbO_3$ doped rear earth ions is a promising material. Pure $LiNbO_3$ and singly doped rear earth ion $LiNbO_3$ show a low threshold for optical damage. It is reported resistant photorefractive effect could be increased with hundredfold by doping Mg^{2+}, Zn^{2+}, In^{3+}, Sc^{3+} and Hf^{4+} ions with their concentration more than their thresholds [16–21]. Mg/Zn:$LiNbO_3$ can improve the ability of photorefractive resistance and decrease the phase-matching temperature [17]. For rear earth Sm^{3+} ion, emissions in the VIS and UV field result from transitions from the sole luminescent state $^4G_{5/2}$ to ground state $^6H_{5/2}$ and excited states $^6H_{7/2}$, $^6H_{9/2}$, $^6H_{11/2}$ and $^6H_{13/2}$. Recently reports about rear earth Sm^{3+} ion contain glasses [22–24] and single crystals such as Sm:$LiNbO_3$ investigated by Dominiak-Dzik [30].

In this paper, we have studied the spectroscopic properties of single crystals Sm^{3+}:$LiNbO_3$ co-doped Mg^{2+} or Zn^{2+}. The polarized transmittance spectra and the Judd–Ofelt theory are applied to determine phenomenological intensity parameters, the radiant transition rates, the total radiant lifetimes, and the branching ratios. The polarized emission spectra are also measured to investigate their fluorescence in visible field.

2. The J–O theory

The Judd–Ofelt theory was developed by Judd [25] and Ofelt [26]. Although the theory and the process of intensity parameter calculation have been applied widely, some related and important formulas are given as followings:

The theoretical electric dipole transition strength from level i to i':

$$S_{ed} = e^2 \sum_{\xi=2,4,6} \Omega\xi |\langle i\|U^{(\xi)}\|i'\rangle|^2 \quad (1)$$

where Ω_ξ signify experimental parameters, $\langle i\|U^{\xi}\|i'\rangle$ is doubly reduced matrix elements of the unit-tensor operator $U^{(\xi)}$, and ξ is only equal to 2, 4 or 6 because of the limit of tensor operator.

The theoretical magnetic dipole transition strength from level i to i':

$$S_{md} = \frac{h^2e^2}{4\pi^2m^2c^2} \sum_{\xi=2,4 \text{ and } 6} \Omega\xi |\langle S_iL_iJ_i\|L + 2S\|S_{i'}L_{i'}J_{i'}\rangle|^2 \quad (2)$$

where $L + 2S$ signify the magnetic dipole operator, m is the mass of electron, h is the Planck constant and c is the light speed in vacuum.

The theoretical transition oscillator strength from level i to i'

$$f_{cal}(i,i') = \frac{8\pi^2mc}{3he^2(2J_i+1)} \frac{(n^2+2)^2}{9n} (S_{ed} + n^3S_{md}) \quad (3)$$

* Corresponding author. Tel.: +86 20 84115692; fax: +86 20 84113293.
E-mail address: wangbiao@mail.sysu.edu.cn (B. Wang).

0925-3467/$ - see front matter © 2011 Elsevier B.V. All rights reserved.
doi:10.1016/j.optmat.2011.11.026

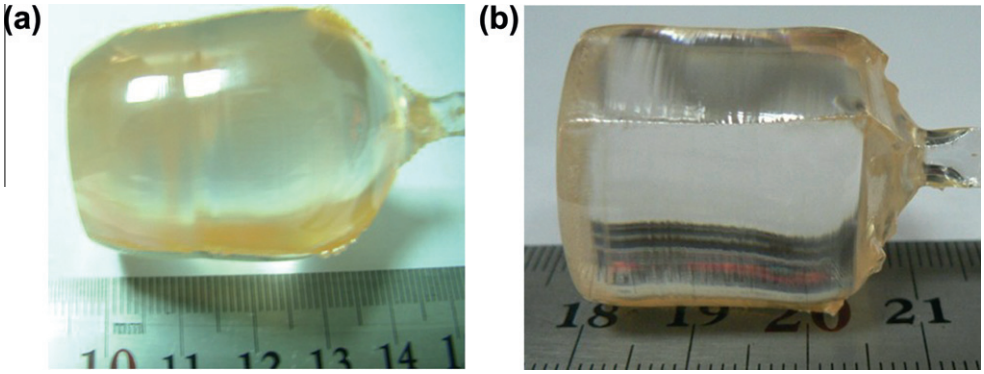

Fig. 1. As-grown and homogeneous single crystals (a) orange Sm:Mg:$LiNbO_3$ with the diameter of 25 mm and the length of 35 mm and (b) orange Sm:Zn:$LiNbO_3$ with the diameter of 20 mm and the length of 25 mm. (For interpretation of the references to color in this figure legend, the reader is referred to the web version of this article.)

where n is the refractive index of the host, λ is the wavelength of transition from level i to i'.

The experimental transition strength can be acquired from the integrated absorption coefficient for each absorption band without considering magnetic dipole, the experimental transition strength from level i to i'.

$$F_{\exp-\gamma} = \frac{mc^2}{N\pi e^2}\int_{\gamma}\alpha(v)dv \tag{4}$$

where $\alpha(v) = \frac{1}{d}\ln(\frac{T0}{T})$, γ relates to σ or π spectrum, T_0 is the transmittance of crystals without rear earth ions and T is the transmittances of crystal doped rear earth ions. N is the active ion's concentration, d is the thickness of the plate and $\alpha(\upsilon)$ is the absorption coefficient.

$$F_{\exp} = \frac{1}{3}(2f_{\exp} - \sigma + f_{\exp} - \pi) \tag{5}$$

Using $f_{\exp} = f_{cal}$, the J–O parameter Ω_ξ and following optical parameters can be calculated.

The root mean-square deviation of the fit:

$$\Delta f_{RMS}(i.i') = \sqrt{\frac{\sum(f^i_{cal} - f^i_{\exp})^2}{p-3}} \tag{6}$$

where p is the number of absorption bands analyzed.

The Einstein emission coefficient:

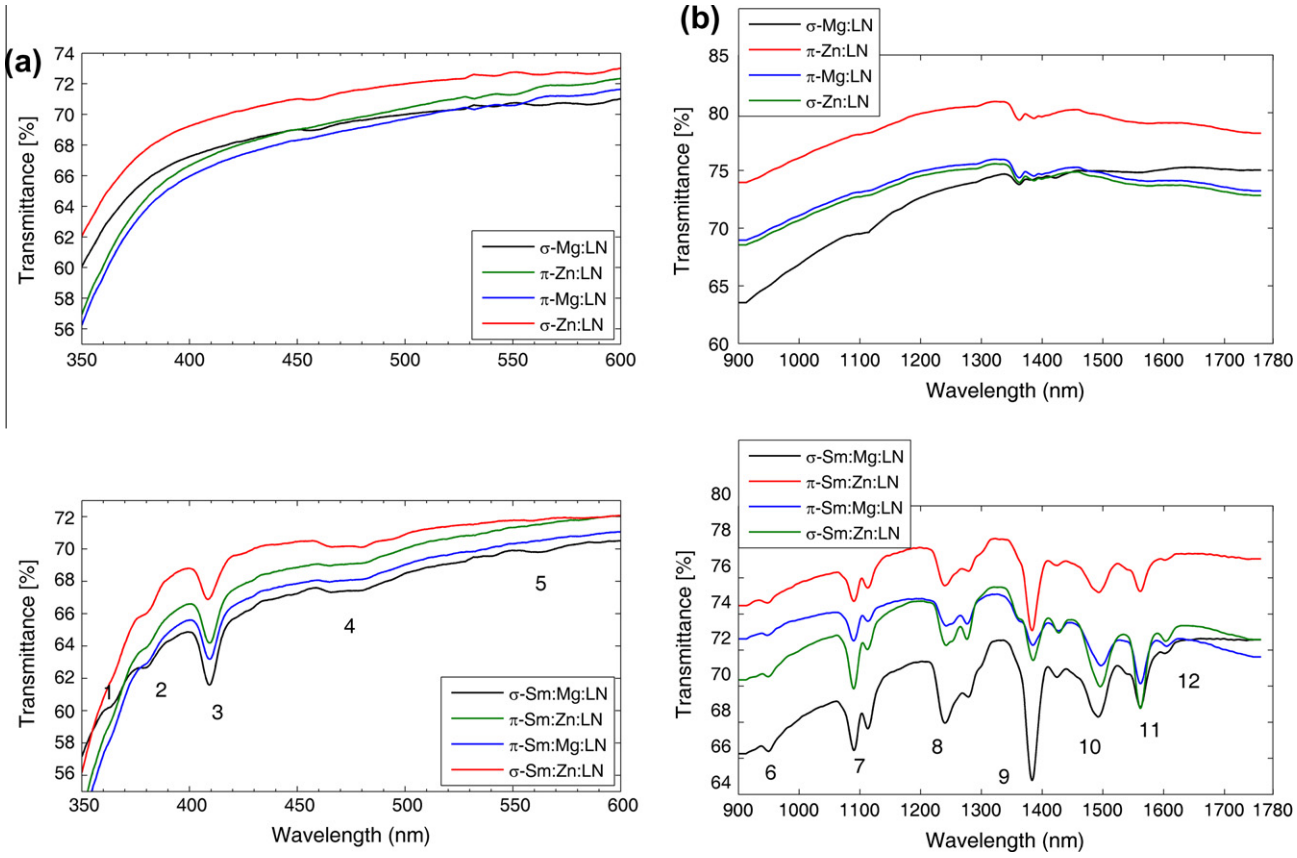

Fig. 2. Polarized transmittance spectra of all crystals (a) Mg/Zn:$LiNbO_3$ and Sm:Mg/Zn:$LiNbO_3$ from 350 to 600 nm and (b) Mg/Zn:$LiNbO_3$ and Sm:Mg/Zn:$LiNbO_3$ from 900 to 1780 nm.

Table 1
Oscillator strengths and Judd–Ofelt parameters of Mg:$LiNbO_3$ and Zn:$LiNbO_3$ doped Sm^{3+}.

Transition from the ground state 6H5/2 →	υ (cm^{-1})	Oscillator strength ($\times10^{-6}$)							
		Sm:Mg:$LiNbO_3$				Sm:Zn:$LiNbO_3$			
		f_σ	f_π	f_{exp}	f_{cal}	f_σ	f_π	f_{exp}	f_{cal}
3	24,450	18.174	5.148	13.832	13.774	16.738	6.656	13.378	13.290
7	9148	4.706	3.106	4.172	3.219	4.786	3.782	4.452	3.020
8	7869	7.542	4.024	6.370	6.928	6.028	5.036	5.698	6.538
9, 10, 11 and 12	6679	19.224	10.984	16.478	16.478	15.146	15.834	15.376	15.376
Judd–Ofelt parameters for Sm:Mg:$LiNbO_3$ ($\times10^{-20}$ cm^2) Ω_2 = 1.860, Ω_4 = 2.824, Ω_6 = 1.194; the root mean square deviation ($\times10^{-7}$ cm^2) Δf_{RMS} = 4.526									
Judd–Ofelt parameters for Sm:Zn:$LiNbO_3$ ($\times10^{-20}$ cm^2) Ω_2 = 1.680, Ω_4 = 2.726, Ω_6 = 1.12; the root mean square deviation ($\times10^{-7}$ cm^2) Δf_{RMS} = 6.80									

For Sm:$LiNbO_3$, the Judd–Ofelt parameters are given by $\Omega_2 = 2.11 \times 10^{-20}cm^2$, $\Omega_4 = 4.50 \times 10^{-20}cm^2$, $\Omega_6 = 1.45 \times 10^{-20}cm^2$ [30]. Here, it is found that the parameters of Sm:Mg/Zn:$LiNbO_3$ increase.

Table 2
The peak wavenumber (ν), radiative transition probability (A_r), branching ratio (β_r), total radiative transition probability (ΣA_r) and radiative lifetime (τ_r).

Transition from 4G5/2 →	υ (cm^{-1})	Sm:Mg:$LiNbO_3$		Sm:Zn:$LiNbO_3$	
		A_r (s^{-1})	β_r	A_r (s^{-1})	β_r
13	17,544	192.5	0.237	184.28	0.241
14	16,467	569.8	0.702	532.01	0.697
15	15,291	49.2	0.061	47.38	0.062
ΣA_r (s^{-1})	811.52			763.66	
τ_r	1232.3			1276.15	

For Sm:$LiNbO_3$, the radiative lifetime is 1122 μs [30]. Here, the results calculated show the radiative lifetimes are enhanced with the values 1232.3 and 1276.15 μs respectively for Mg and Zn doped Sm:$LiNbO_3$.

$$A_r(i,i') = \frac{64\pi^4 e^2}{3h(2J_i+1)} \frac{n(n^2+2)^2}{9} \frac{1}{\lambda} S_{ed} \tag{7}$$

The excited state radiant lifetime:

$$\tau = \frac{1}{\sum A_r(i,i')} \tag{8}$$

The fluorescence branching ration:

$$\beta(i,i') = \tau \times A_r(i,i') \tag{9}$$

3. Experiments details

All congruent (Li/Nb = 0.945) single crystals containing Sm : Mg (5 mol%):$LiNbO_3$, Sm:Zn(6.5 mol%):$LiNbO_3$, Mg(5 mol%):$LiNbO_3$ and Zn(6.5 mol%):$LiNbO_3$ were prepared by Czochralski technique. Shown in Fig. 1, uniform and high-quality crystals have been grown. The nominal concentration of Sm^{3+} ions is 0.3 mol%. Oriented crystals were cut into wafers with planes of polarization perpendicular to and parallel to c-axis, and samples cut were labeled σ and π correspondingly. The polarized absorption spectra were recorded by UV–VIS-NIR spectrophotometer at room temperature. To determine the optical properties of Sm:Mg:$LiNbO_3$ and Sm:Zn:$LiNbO_3$, the polarized transmittance spectra of matrixes containing Mg:$LiNbO_3$ and Zn:$LiNbO_3$ were also measured at the same conditions. The polarized emission spectra were obtained by *RF*-5301 spectrofluorophotometer.

4. Results and discussion

Fig. 2 presents polarized transmittance spectra of all crystals from 350 nm to 600 nm and from 900 nm to 1780 nm. The absorption coefficient is calculated by the formula $\alpha(\nu) = \frac{1}{d} \ln\left(\frac{T_0}{T}\right)$. From the transmittance spectra, various optical transitions of Sm^{3+} are observed because of complicated stark energy levels which are formed by crystal field with the C_3 symmetry of $LiNbO_3$. For Sm^{3+}, all transitions observed are predominantly induced by electric dipoles. From formulas (4) and (5), f_{exp} is acquired and tabulated in Table 1. For f_{cal}, refractive indices of hosts including Mg:$LiNbO_3$ and Zn:$LiNbO_3$ have been measured respectively by Shen et al. [27] and Nevado et al. [28], and the matrix elements $\langle i\|U^\xi\|i'\rangle$ are quoted from results reported for Sm^{3+} in LaF_3 by Carnall et al. [29]. Using formula (3), the J–O phenomenological parameters Ω_2, Ω_4 and Ω_6 are given by least-squares-fitting methods, and f_{cal} is calculated and presented in Table 1. Using formulas (6), the root mean-square deviations are given and shown in Table 1. By using formulas (7)–(9), the Einstein emission coefficient A_r, the excited state radiant lifetime τ_r and the fluorescence branching ratio β are calculated and tabulated in Table 2 too. For Sm:$LiNbO_3$ single crystals, the Judd–Ofelt parameters are given by $\Omega_2 = 2.11 \times 10^{-20}$ cm^2, $\Omega_4 = 4.50 \times 10^{-20}$ cm^2, $\Omega_6 = 1.45 \times 10^{-20}$ cm^2, that indicates the relation with $\Omega_4 > \Omega_2 > \Omega_6$ occurs [30]. Here, in Table 1 it is found the relation still exists in both of Sm:Mg:$LiNbO_3$ and Sm:Zn:$LiNbO_3$ crystals. From Table 1, Ω_2 as well as $\Sigma\Omega_\xi$ in Sm:Zn:$LiNbO_3$ decreases compared with that of Sm:Mg:$LiNbO_3$, the results indicate the covalent chemical bonding of Sm^{3+} in Mg/ Zn:$LiNbO_3$ changed, owing to the differences of electro-negativity between Mg and Zn. The radiant lifetimes of excited state τ_r are calculated and given by the values 1232.3 and 1276.15 μs respectively for Mg/Zn:$LiNbO_3$, the results show the

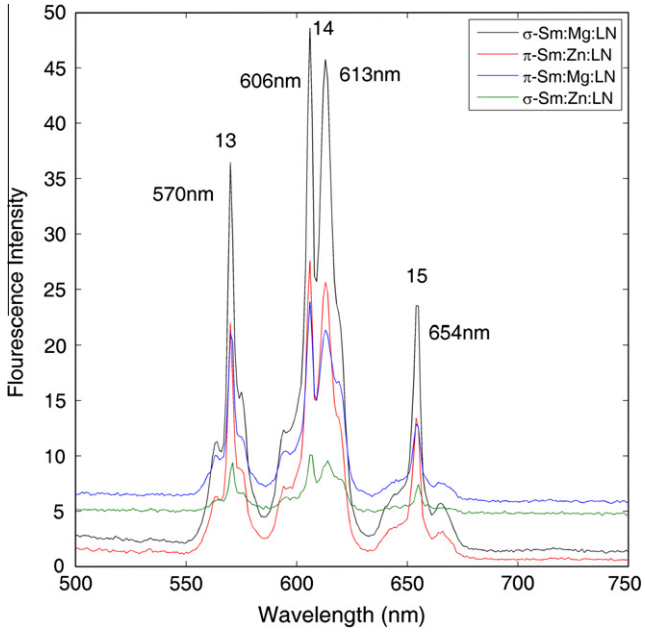

Fig. 3. Polarized emission spectra of Sm:Mg/Zn:$LiNbO_3$ under 409 nm excitation.

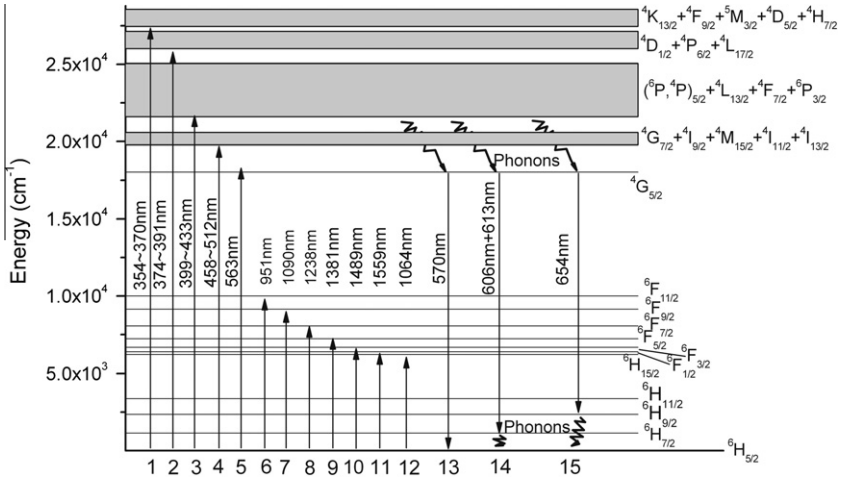

Fig. 4. Simplified energy levels diagram for Sm:Mg/Zn:$LiNbO_3$.

lifetime is long, which is also found in Sm:$LiNbO_3$ with the value 1122 μs [30]. The fluorescence branching ratios β of transitions $^4G_{5/2} \rightarrow {}^6H_{5/2}$ and $^4G_{5/2} \rightarrow {}^6H_{9/2}$ are about the same values in both of crystals, but the ratio of transition $^4G_{5/2} \rightarrow {}^6H_{7/2}$ in Sm^{3+}:Mg:$LiNbO_3$ is higher than that in Sm^{3+}:Zn:$LiNbO_3$.

The most intense absorption peak 409 nm is corresponding to transitions from ground state $^6H_{5/2}$ to excited states $(^6P, {}^4P)_{5/2}$, $^4L_{13/2}$, $^4F_{7/2}$ and $^6P_{3/2}$. So the wavelength of 409 nm can be used as the excitation wavelength to acquire fluorescence. In Fig. 3, the polarized emission spectra were recorded under the 409 nm excitation. Most intense lines are at 606 and 613 nm, because the state $^6H_{7/2}$ is split into stark energies owing to crystal field. The centered peak wavelengths of 570 and 654 nm are corresponding to dominant transitions from the fluorescent state $^4G_{5/2}$ to excited states $^6H_{5/2}$ and $^6H_{9/2}$. The ratios of polarized emission intensities integrated along wave number are expressed as the following formula:

$$\int_{v_1}^{v_2} \rho_{570\mathrm{nm}}(v)dv : \int_{v_3}^{v_4} \rho_{606+613\mathrm{nm}}(v)dv : \int_{v_5}^{v_6} \rho_{654\mathrm{nm}}(v)dv = \int_{v_1}^{v_2} I_{570\mathrm{nm}}(v)dv : \int_{v_3}^{v_4} I_{606+613\mathrm{nm}}(v)dv : \int_{v_5}^{v_6} I_{654\mathrm{nm}}(v)dv$$

where $\rho(\upsilon)$ is energy density, $I(\upsilon)$ is fluorescent intensity, υ_1, υ_2, υ_3, υ_4, υ_5 and υ_6 are respectively 18,149, 17,065, 17,055, 15,798, 15,785 and 14728 cm^{-1}. Integrated results of π and σ Sm:Mg:$LiNbO_3$ as well as π and σ Sm:Zn:$LiNbO_3$ are correspondingly 1:2.76:0.807, 1:2.64:0.652, 1:2.78:0.803 and 1:2.75:0.768. All transitions of absorption and emission are schematized in Fig. 4. Multiple-phonon nonradiative relaxation enhances emission efficiency from pumping bands $(^6P, {}^4P)_{5/2}$, $^4L_{13/2}$, $^4F_{7/2}$ and $^6P_{3/2}$ to fluorescent state $^4G_{5/2}$ and from excited states $^6H_{7/2}$ and $^6H_{9/2}$ to the ground state $^6H_{5/2}$.

5. Conclusion

The Judd–Ofelt intensity parameters (Ω_2, Ω_4 and Ω_6) have been calculated for Sm:Mg:$LiNbO_3$ and Sm:Zn:$LiNbO_3$. Results present that Ω_2 and $\Sigma\Omega_\xi$ (ξ = 2, 4 and 6) of Sm^{3+} doped Zn:$LiNbO_3$ decrease because local covalent environments change between Sm^{3+} and the matrix. The excited state radiant lifetimes τ_r of crystals doubly doped Sm^{3+} and refractive resistant ions Mg^{2+} and Zn^{2+} are respectively 1232.3 and 1276.15 μs. Fluorescent emission spectra indicate that visible fluorescence of Sm^{3+} consists of green light 570 nm, orange bands 605 and 613 nm and reddish-orange light 654 nm under 409 nm excitation in both of Sm:Mg:$LiNbO_3$ and Sm:Zn:$LiNbO_3$ crystals. Above results indicate that it is possible to develop Sm^{3+} doped Mg or Zn:$LiNbO_3$ crystals as laser materials at 606 nm or 613 nm pumped by UV laser diodes.

Acknowledgment

This paper is sponsored by the National Natural Science Foundation of China (Grant Nos. 10972239, 10732100 and 11072271).

References

[1] Y. Furukawa, K. Kitamura, S. Takekawa, K. Niwa, Y. Yajima, N. Iyi, I. Mnushkina, P. Guggenheim, J.M. Martin, J. Cryst. Growth 211 (2000) 230–236.
[2] J.K. Yamamoto, T. Yamazaki, K. Yamaishi, Appl. Phys. Lett. 64 (24) (1994) 3228–3230.
[3] L.E. Myers, G.D. Miller, R.C. Eckardt, M.M. Fejer, R.L. Byer, W.R. Bosenberg, Opt. Lett. 20 (1995) 52–54.
[4] R. Piramidowicz, I. Pracka, W. Wolinski, M. Malinowski, J. Phys.: Condens. Matter. 12 (2000) 709–718.
[5] A. Lorenzo, E. Camarillo, H.S. Murrieta, E. Alvarez, U.G. Caldino, J.A. Hernandez, M. Voda, F. Jaque, J. Garcia Sole, Opt. Mater. 5 (1996) 251–258.
[6] A. Lorenzo, L.E. Bausa, J.A. Sanz Garcia, J. Garcia Sole, J. Phys.: Condens. Matter. 8 (1996) 5781–5791.
[7] A.H. Li, L. Sun, Z.R. Zheng, W.L. Liu, W.Z. Wu, Y.Q. Yang, T.Q. Lv, Appl. Phys. A. 89 (2007) 1005–1010.
[8] Y.F. Ruan, X.M. Wang, T. Tsuboi, J. Alloys Compd. 246 (1998) 275–277.
[9] A. Arcangeli, D. Parisi, A. Toncelli, M. Tonelli, M. Bazzan, N. Argiolas, M.V. Ciampolillo, C. Sada, J. Appl. Phys 104 (2008) 103114–103114-6.
[10] E. Cantelar, G.A. Torchia, F. Cusso, J. Lumin. 122 (2007) 459–462.
[11] T. Tsuboi, S.M. Kaczmarek, G. Boulon, J.Alloys Compd. 380 (2004) 196–200.
[12] M. Nakamura, M. Sekita, S. Takekawa, K. Kitamura, J. Cryst. Growth. 290 (2006) 144–148.
[13] J.K. Yamamoto, A. Sugimoto, K. Yamagishi, Opt. Lett. 19 (1994) 1311–1313.
[14] J.N.B. Reddy, K.G. Kamath, S. Vanishri, H.L. Bhat, S. Elizabeth, J. Chem. Phys. 128 (2008) 244709.
[15] M. Quintanilla, E. Cantelar, J.A. Sanz-Garcia, F. Cusso, Opt. Mater. 30 (2008) 1089–1102.
[16] D.A. Bryan, R. Gerson, H.E. Tomaschke, Appl. Phys. Lett. 44 (1984) 847–849.
[17] T.R. Volk, V.I. Pryalkin, N.M. Rubinina, Opt. Lett. 15 (1990) 996–998.
[18] Haijun Qiao, Jingjun Xu, Qiang Wu, Xuanyi Yu, Qian Sun, Xinzheng Zhang, Guangyi Zhang, T.R. Volk, Opt. Mater. 23 (2003) 269–272.
[19] Yonfa Kong, Jinke Wen, Huafu Wang, Appl. Phys. Lett. 66 (1995) 280–281.
[20] J.K. Yamamoto, K. Kitamura, N. Iyi, S. Kimura, J. Cryst Growth. 121 (1992) 522–526.
[21] Shuqi Li, Shiguo Liu, Yonfa Kong, Donglin Deng, Guanyu Gao, Yanbo Li, Hongchen Gao, Ling Zhang, Ziheng Huang, Shaolin Chen, Jingjun Xu, J. Phys.: Condens. Matter. 18 (2006) 3527–3534.
[22] P. Raghava Rao, G. Murali Krishna, M.G. Brik, Y. Gandi, N. Veeraiah, J. Lumin. 131 (2011) 212–217.
[23] R. Praveena, V. Venkatramu, P. Babu, C.K. Jayasankar, T. Troster, W. Sievers, G. Wortmann, J. Phys.: Condens. Matter 21 (2009) 035108.

[24] A.G. Souza Filho, J. Mendes Filho, F.E.A. Melo, M.C.C. Custodio, R. Lebullenger, A.C. Hernandes, J. Phys. Chem. Solids 61 (2000) 1535–1542.
[25] B.R. Judd, Phys. Rev. 127 (1962) 750–761.
[26] G.S. Ofelt, J. Chem. Phys. 37 (1962) 511–521.
[27] H.Y. Shen, H. Xu, Z.D. Zeng, W.X. Lin, R.F. Wu, G.F. Xu, Appl. Opt. 29 (1992) 1281–1283.
[28] R. Nevado, G. Lifante, G.A. Torchia, J.A. Sanz-Garcia, F. Jaque, Opt. Mater. 11 (1998) 35–40.
[29] W.T. Carnall, H. Crosswhite, H.M. Crosswhite, Energy Level Structure and Transition Probabilities in the Spectra of the Trivalent Lanthnides in LaF3 – Annual Report, Argonne National Laboratory, 1975.
[30] G. Dominiak-Dzik, J. Alloys Compd. 391 (2005) 26–32.